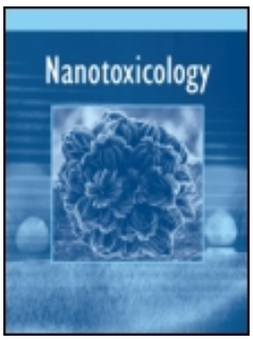

Nanotoxicology

ISSN: 1743-5390 (Print) 1743-5404 (Online) Journal homepage: https://www.tandfonline.com/loi/inan20

Size and surface charge significantly influence the toxicity of silica and dendritic nanoparticles

Khaled Greish, Giridhar Thiagarajan, Heather Herd, Robert Price, Hillevi Bauer, Dallin Hubbard, Alexander Burckle, Shraddha Sadekar, Tian Yu, Arnida Anwar, Abhijit Ray & Hamidreza Ghandehari

To cite this article: Khaled Greish, Giridhar Thiagarajan, Heather Herd, Robert Price, Hillevi Bauer, Dallin Hubbard, Alexander Burckle, Shraddha Sadekar, Tian Yu, Arnida Anwar, Abhijit Ray & Hamidreza Ghandehari (2012) Size and surface charge significantly influence the toxicity of silica and dendritic nanoparticles, Nanotoxicology, 6:7, 713-723, DOI: 10.3109/17435390.2011.604442

To link to this article: https://doi.org/10.3109/17435390.2011.604442

Nanotoxicology, November 2012; 6(7):713–723

ISSN: 1743-5390 print / 1743-5404 online
DOI: 10.3109/17435390.2011.604442

informa
healthcare

Size and surface charge significantly influence the toxicity of silica and dendritic nanoparticles

Khaled Greish[1,2,#], Giridhar Thiagarajan[2,3,#], Heather Herd[2,3], Robert Price[1,2], Hillevi Bauer[1,2], Dallin Hubbard[2,3], Alexander Burckle[2,3], Shraddha Sadekar[1,2], Tian Yu[1,2], Arnida Anwar[1,2], Abhijit Ray[1,2] & Hamidreza Ghandehari[1,2,3]

[1]Department of Pharmaceutics and Pharmaceutical Chemistry, University of Utah, Salt Lake City, UT, USA, [2]Utah Center for Nanomedicine, Nano Institute of Utah, University of Utah, Salt Lake City, UT, USA and [3]Department of Bioengineering, University of Utah, Salt Lake City, UT, USA

Abstract

The influence of size, surface charge and surface functionality of poly(amido amine) dendrimers and silica nanoparticles (SNPs) on their toxicity was studied in immunocompetent mice. After systematic characterization of nanoparticles, they were administered to CD-1 (caesarean derived-1) mice to evaluate acute toxicity. A distinct trend in nanotoxicity based on surface charge and functional group was observed with dendrimers regardless of their size. Amine-terminated dendrimers were fatal at doses >10 mg/kg causing haematological complications such as disseminated intravascular coagulation-like manifestations whereas carboxyl- and hydroxyl-terminated dendrimers of similar sizes were tolerated at 50-fold higher doses. In contrast, larger SNPs were less tolerated than smaller SNPs irrespective of their surface functionality. These findings have important implications in the use of these nanoparticles for various biomedical applications.

Keywords: Nanotoxicity, silica nanoparticles, PAMAM dendrimers, disseminated intravascular coagulation, biocompatibility

Introduction

The last few decades have witnessed advances in nanotechnology with unprecedented precision in manufacturing of well-defined nanomaterials for diverse applications such as semiconductors, cosmetics and biomedical systems (Fruijtier-Polloth 2005; Hardman 2006; Nel et al. 2006). As is true for any emerging technology with potential biomedical applications, careful assessment of toxicities and biological interactions is essential. However, most toxicity assessments of nanomaterials have so far been conducted in cultured cells with very few comprehensive studies *in vivo*. *In vitro* data from these studies could be misleading and further verification in animal models is critical (Fischer & Chan 2007). *In vivo* systems are extremely complex and interaction of nanostructures with biological components such as blood, circulating proteins and immune factors could lead to unique biological outcomes that cannot be captured in isolated *in vitro* experiments. Understanding the relationship between the physicochemical properties of nanostructures and their *in vivo* behaviour can provide predictive models for assessing human toxicity (Aillon et al. 2009). In the current study, we chose two commonly used representative nanostructures, namely silica nanoparticles (SNPs), and poly (amido amine) (PAMAM) dendrimers, for evaluating the influence of physicochemical properties such as core composition, size, surface charge and surface-functional groups on toxicity *in vivo*.

Silica-based nanoparticles are increasingly being used in biomedical and biotechnological applications such as biosensors, biomarkers and drug delivery vehicles (Lin et al. 2006) since they can be easily surface-modified (Weetall 1993) for ligand attachment and are extremely stable exhibiting no swelling or changes in porosity with pH or temperature. SNPs can be engineered under simple and ambient conditions (Weetall 1993) to produce the desired size, shape and porosity. SNPs also have extensive applications in chemical and mechanical polishing, food and drug additives and semiconductor industry. Hence, the environmental and health impact of SNPs is of great concern.

Dendritic nanostructures also have broad applications in the fields of electronics, bioseparation, petroleum and superconductors (Service 1995) as well as in potential biomedical applications such as drug delivery and diagnostic imaging (Svenson & Tomalia 2005; Wilbur et al. 1998). The precision to incrementally increase the size and number of selective surface-functional groups make dendrimers suitable candidates for such applications. PAMAM dendrimers have a

Correspondence: Hamidreza Ghandehari, Utah Center for Nanomedicine, Nano Institute of Utah, University of Utah, Salt Lake City, UT 84108, USA. Tel: +(001) 801 587 1566. Fax: +(001) 801 585 0575. E-mail: hamid.ghandehari@pharm.utah.edu
# These authors contributed equally to this work.

(Received 29 December 2010; accepted 5 July 2011)

unique tree-like branched architecture, near spherical shape in solution (Tomalia 1994; Tomalia et al. 1990) and narrow polydispersity indices ~1.000002 to 1.005 (Esfand & Tomalia 2001). The high density of surface functional groups and the ability to easily manipulate functionality through simple organic reactions have led to their extensive use. Even though both SNPs and PAMAM dendrimers hold promise in biomedical applications, minimal *in vivo*, safety assessments have been performed with these nanoconstructs. The purpose of the current investigation is to evaluate the safety of PAMAM dendrimers and SNPs as a function of size, surface charge and core composition in immunocompetent mice.

Methods

Preparation of SNPs

Non-porous SNPs of approximately 50 and 200 nanometres in diameter were synthesized utilizing the Stober method (Stober et al. 1968). Following synthesis, a reactive 3-aminopropyltriethoxysilane (Gelest, Morrisville, PA, USA) was coupled to the silica surface to provide surface amine functionalization as reported earlier (Van Blaaderen & Vrij 1992). After the synthesis, each batch of particles was washed three times with ethanol and deionized water followed by a final ethanol wash. The particles were then dried in an oven at 80°C overnight, weighed and placed in sterilized glass vials. The vials containing SNPs were dried by autoclave and stored at room temperature. The size and shape of approximately 300 particles of each construct were determined by transmission electron microscopy (Phillips TECHAI F2, Hillsboro, OR) at an accelerating voltage of 80 kV. Zeta potentials and sizes of the constructs were measured by dynamic light scattering (DLS) at concentrations of 1 mg/ml at pH 7.4 (non-buffered) in triplicates using a Malvern Instruments Zetasizer Nano ZS (Westborough, MA, USA). The Zetasizer Nano ZS was equipped with an electronic titrator to perform subsequent titrations of each construct and evaluate the number of terminal functional groups on the surface of nanoparticles (Supplementary Table I). Each titration was performed with a concentration of 7 mg/ml of constructs with 1 M HCl titrant. Following titration, the equivalence point was determined via the second derivative of the obtained titration curve.

Preparation of PAMAM dendrimers

PAMAM dendrimers of different generations (G) were purchased from Sigma (St Louis, MO, USA). Dendrimer samples were further fractionated by a preparative Sephadex Hiload 75 size exclusion column as necessary to remove small molecular weight impurities (Figure 1E and Supplementary Figure 1). All dendrimers were characterized at physiologically relevant pH by DLS at a concentration of 5 mg/ml and their zeta potential recorded on a Malvern Zetasizer at a concentration of 10 mg/ml in triplicates. In addition, PAMAM dendrimers were characterized by high-performance liquid chromatography and size exclusion chromatography (SEC) on an analytical Superose 6 10/300 GL column (GE Healthcare, Piscataway, NJ). Elution buffer was phosphate-buffered saline (PBS): acetonitrile (80:20) with 0.1% sodium azide.

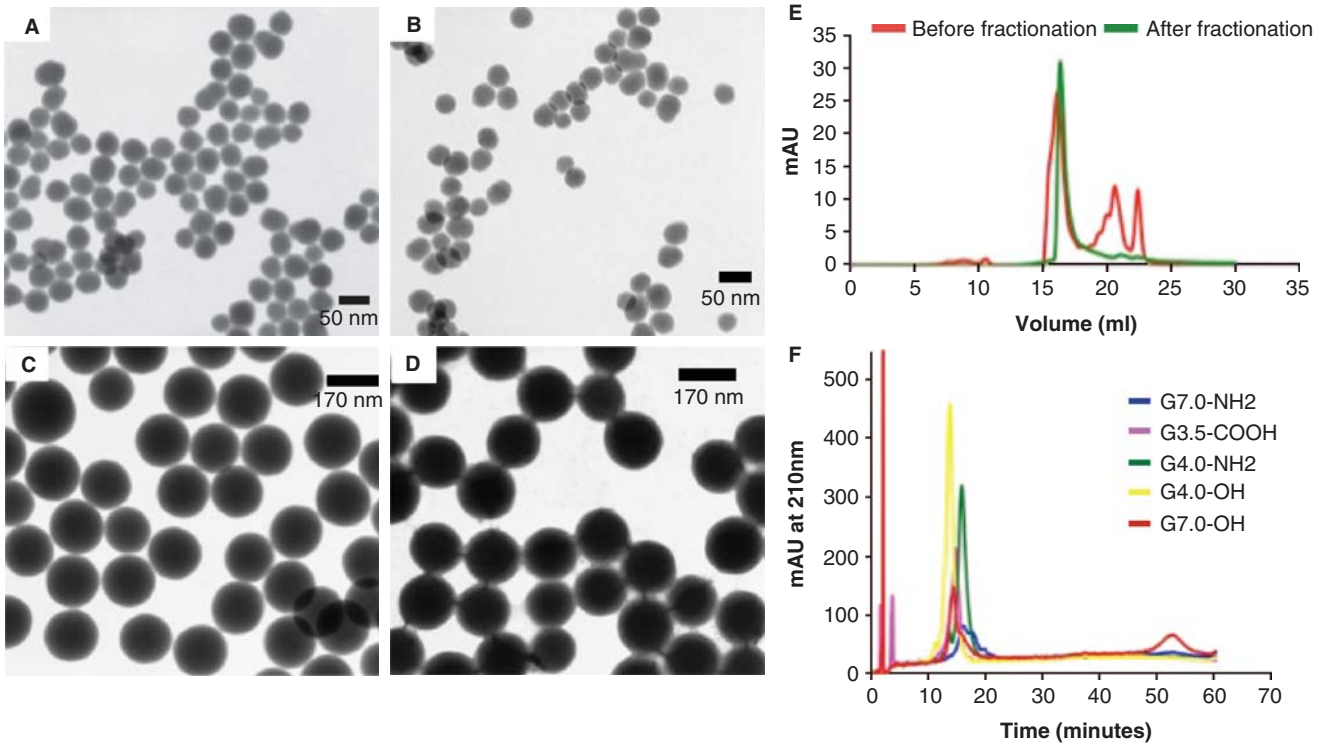

Figure 1. Characterization of nanoconstructs. Transmission electron microscopic images of: A) 50-nm silica nanoparticles with hydroxyl surface groups; B) 50-nm silica nanoparticles with amine surface groups; C) 200-nm silica nanoparticles with amine surface groups; D) 200-nm silica nanoparticles with hydroxyl surface groups; E) size exclusion profile (SEC) of G7-NH_2 dendrimers on a Superose 6 column showing small molecular impurities before fractionation; and F) high-performance liquid chromatography (HPLC) chromatograms of PAMAM dendrimer probes on C18 column.

In vivo acute toxicity studies

Animals

Both mice and rats were employed in evaluating toxicity. All acute toxicity studies were carried out in 4- to 6-week-old female caesarean derived-1 (CD-1) mice. *In vivo* coagulation and fibrinolysis were studied in female Sprague–Dawley (SD) rats weighing about 150–200 g. Both strains were purchased from Charles River Laboratories (Boston, MA, USA) and used according to the rules and guidelines of the University of Utah Institutional Animal Care and Use Committee.

Study design

To measure acute toxicity, single escalating doses were administered starting from 3 to 1 mg/kg at half-log dose increments (Table I). Five CD-1 mice were randomly assigned to a group to test each dose of the nanoparticles. A separate control group was also assigned. Maximum tolerated dose (MTD) was considered as the maximum dosage of a particular nanoparticle that resulted in <10% animal weight loss over a period of 10 days. At a given dose of a particular nanoparticle when overt toxicity is observed [>10% animal weight loss or other clinical signs of toxicity (Supplementary Table II)], the animal was humanly euthanized by CO_2 asphyxiation and the dosage of that particular nanoparticle was reduced to midway between the current lethal dose and earlier determined maximum dose that was tolerated.

Nanoconstruct administration and follow-up

All tested compounds were dispersed in sterile physiological saline. Samples were filtered through 0.2-μm filters and injected intravenously (i.v.) by tail vein injections to CD-1 mice at 0.2 ml/mice. To exclude the presence of endotoxin in nanoparticle samples, an endpoint Limulus Amebocyte Lysate (LAL) assay (QCL-1000; Lonza, Walkersville, MD) was performed according to the manufacturer's instructions. Briefly, 50 μl of nanoconstruct sample and a standard *Escherichia coli* endotoxin were each mixed with 50 μl of LAL in a microplate at 37°C and incubated for 10 min. Then 100 μl of substrate solution (Ac-lle-Glu-Ala-Arg-pNA) was added and incubated at 37°C for an additional 6 min. About 100 μl stop reagent (25% glacial acid in H_2O) was subsequently added and the plates read at 405 nm (SoftMax Pro; Molecular Devices, Sunnyvale, CA). Immediately after injections, animals were observed for 30 min for post-injection reaction. Animal weight was recorded and systemic clinical observations were carried out twice daily for a period of 10 days (Supplementary Table II). When signs of toxicity were observed during clinical observation or animals lost more than 10% of body weight, they were humanely euthanized.

Euthanization, tissue and blood analysis

Ten days after injection, mice were individually euthanized using 70% CO_2 in oxygen, with euthanasia confirmed by lack of breathing for 10 s. Blood was taken via inferior vena cava (IVC) stick, and drawn into a heparinized syringe through a 23G needle and deposited into a heparinized plastic blood tube. Blood samples were examined for clotting and/or haemolysis upon collection. Organs [heart, lungs, liver, spleen, kidney and gastrointestinal (GI) tract] were removed, weighed and % weight of organ to total body weight calculated to determine organ atrophy/hypertrophy in response to nanoparticle injection. Liver and kidneys of animals showing abnormality were further examined by histological

Table I. Acute toxicity observations in CD-1 mice.

Treatment group	No. of CD-1 mice	No. of deaths	Immediate toxicity
SNP-NH_2 (50 nm)			
10 mg/kg	5	0	No
30 mg/kg	5	0	No
100 mg/kg	5	0	No
150 mg/kg	5	0	No
200 mg/kg	1	1	Yes
300 mg/kg	1	1	Yes
SNP-OH (50 nm)			
10 mg/kg	5	0	No
30 mg/kg	5	0	No
100 mg/kg	5	0	No
150 mg/kg	5	0	No
200 mg/kg	5	0	No
300 mg/kg	2	2	Yes
SNP-NH_2 (200 nm)			
10 mg/kg	5	0	No
30 mg/kg	5	0	No
SNP-OH (200 nm)			
10 mg/kg	5	0	No
30 mg/kg	5	0	No
G7-NH_2			
3 mg/kg	5	0	No
10 mg/kg	5	1	Yes
30 mg/kg	5	5	Yes
G7-OH			
10 mg/kg	5	0	No
30 mg/kg	5	0	No
100 mg/kg	5	0	No
300 mg/kg	5	0	No
1000 mg/kg	5	0	No
G 6.5-COOH			
10 mg/kg	5	0	No
30 mg/kg	5	0	No
100 mg/kg	5	0	No
300 mg/kg	5	0	No
500 mg/kg	5	0	No
1000 mg/kg	2	1	Yes
G4-NH_2			
10 mg/kg	5	0	No
30 mg/kg	5	4	Yes
G4-OH			
10 mg/kg	5	0	No
30 mg/kg	5	0	No
100 mg/kg	5	0	No
300 mg/kg	5	0	No
500 mg/kg	5	0	No
1000 mg/kg	2	1	Yes
G3.5-COOH			
10 mg/kg	5	0	No
30 mg/kg	5	0	No
100 mg/kg	5	0	No
300 mg/kg	5	0	No
1000 mg/kg	5	0	No

sectioning and H&E staining. Complete blood counts (CBCs) were performed within 2 h of blood collection using a CBC-DIFF (Heska, Loveland, CO, USA) blood count analyser. Following CBC, samples were centrifuged at 10,000 rpm for 2.5 min. To examine kidney and liver toxicity, the collected serum samples were used to measure blood urea nitrogen (BUN), creatinine, aspartate aminotransferase (AST), alanine aminotransferase (ALT), total bilirubin, total protein and albumin using a DRI-CHEM (Heska) veterinary blood chemistry analyser. CD-1 mice administered with a dose of >10 mg/kg of amine-terminated dendrimers (both G7 and G4) showed extensive clotting associated with imminent lethality, thus blood collection yields were lesser than optimal in order to perform the blood analysis. For this reason and to specifically examine blood coagulation/fibrinolysis, female SD rats (n = 3) were injected with amine-terminated G4 and G7 at 30 mg/kg. Then after 30 min, animals were euthanized and blood was collected as mentioned above and examined for fibrinogen levels, platelet counts and fibrin degradation products (FDPs).

Oral administration of PAMAM dendrimers

To evaluate acute toxicity after oral administration of PAMAM dendrimers, 4- to 6-week-old female CD-1 mice (n = 5) were used. Each dose of PAMAM dendrimer or saline control was prepared similar to i.v. doses in a total volume of 0.2 ml/mice with physiological saline. Each dose was administered by oral gavage using appropriately sized, curved feeding needles. Unless animals showed signs of toxicity (as mentioned in '*In vivo* acute toxicity studies' section), the acute toxicity study progressed to completion (10-day period). At the end of the study, animals were sacrificed and other toxicity parameters were analysed as mentioned in '*In vivo* acute toxicity studies' section. MTDs were determined in a similar fashion to i.v. doses. All rules and guidelines of the University of Utah Institutional Animal Care and Use Committee were followed.

Human blood experiments

Human blood was collected from donors after Institutional Review Board (IRB) approval. About 20 ml of blood were collected from each donor and divided into three parts. To each part, 0.2 ml of either amine-terminated G4, amine-terminated G7 (a dose comparable to 30 mg/kg) or normal saline as a control was added. Each tube was incubated at 37°C for 10 min with 70 rpm shaking, followed by platelet count and measurement of fibrinogen level and FDP.

Biodistribution of PAMAM dendrimers

CD-1 mice (4–6 weeks old) were employed in the biodistribution studies. Before administration, ^{125}I-labeled dendrimers (G7-NH_2, G7-OH, G6.5-COOH and G4-NH_2) were characterized by SEC (PD-10) to ensure the absence of small molecular weight impurities. Doses below the toxic range (~1 mg/kg, as determined from the toxicity studies) were administered by i.v. tail vein injection (n = 5). Radioactive dosage was adjusted to be ~200,000 CPM/mice in saline solution and a maximum of 0.2 ml/mice was administered. All animal experiments were performed according to the University of Utah, IACUC regulations. Animals were housed in metabolic cages to facilitate the collection of urine and stool samples. They were fed normal diet during the study. At each time point (2 h, 8 h), animals were euthanized with CO_2 and their blood collected immediately. Animals were flushed with saline and subsequently liver, kidney, GI tract, spleen, brain, thyroid, lungs, heart and gall bladder were collected into scintillating vials. Radioactivity present in each organ was measured by γ-counter. Graphs of biodistribution were presented as a percentage of total doses recovered from animals. Radioactivity in blood was normalized to weight.

Protein opsonization studies

Stock solutions of bovine serum albumin (BSA) (10 μmol/l) and PAMAM dendrimers (160 μmol/l) both G7-NH_2 and G6.5-COOH were prepared in PBS (pH 7.4). PAMAM dendrimers were serially diluted to study their interaction with BSA at a concentration range of 2.5–80 μmol/l for PAMAM and 5 μmol/l for BSA. Fluorescence quenching was studied in a 96-well black plate (Nalge Nunc International, Rochester, NY, USA) and samples were excited at 280 nm and emission spectra recorded from 300 to 500 nm on a SpectraMax® M2 (Molecular Devices Corporation, Sunnyvale, CA, USA). Quenching data were collected for BSA, PAMAM and BSA plus PAMAM at varying concentrations.

Statistical analysis

Statistical differences in the levels of blood coagulation indicators between different treatment groups was analysed by a Student's t-test using Microsoft Excel and GraphPad Prism 5.01 software (GraphPad Software, Inc., La Jolla, CA, USA). Significant difference was defined as $p < 0.05$ and highly significant was defined as $p < 0.01$.

Results

PAMAM dendrimers and SNPs of various sizes and surface functionalization were prepared and characterized. Characteristics of the nanoconstructs that were employed in subsequent *in vivo* studies are shown in Table II and Figure 1. With respect to dendrimers, the effect of size on toxicity was studied by comparing two different generations whereas the effect of surface charge and functional group was evaluated by comparing dendrimers of the same generation (similar size) but with amine-, carboxyl-, or hydroxyl-terminal groups. We also evaluated two size ranges of SNPs (50 and 200 nm) each in turn having two surface functionalities (hydroxyl and amine). In total, we evaluated the toxicity profile of 10 different nanoconstructs.

In vivo toxicity as a function of nanoparticle size and surface charge

MTDs were established for each nanoconstruct by half-log dose escalations starting at 1 mg/kg until animals showed >10% weight loss or if overt signs of toxicity were observed. Results indicate a distinct trend in the observed MTDs for PAMAM dendrimers and SNPs (Figure 2). All used nanoconstructs in the study were tested and endotoxin contaminations were not detected.

Table II. Physicochemical characterization of nanoconstructs.

Nanoconstruct	Surface functional group	No. of surface groups	Size (diameter) in nm	Zeta potential (mV)
G 3.5	COOH	64[a]	3.2 ± 0	[b]
G 4	NH_2	64[a]	3.4 ± 0.22	[b]
G 4	OH	64[a]	2.6 ± 0	[b]
G 6.5	COOH	512[a]	8.5 ± 0.61	−42.0 ± 1.2[c]
G 7	NH_2	512[a]	8.1 ± 0.42	64.8 ± 3.2[c]
G7	OH	512[a]	6.4 ± 0	27.7 ± 1.1[c]
SNP (50 nm)	NH_2	1466[d]	48.2 ± 5.1	-17.6 ± 9.5[c]
SNP (50 nm)	OH	36,891[d]	48.6 ± 4.5	-61 ± 8.6[c]
SNP (200 nm)	NH_2	6,089[d]	173.6 ± 13.2	46 ± 17.5[c]
SNP (200 nm)	OH	66,3214[d]	165.3 ± 12.6	-72 ± 19.1[c]

[a]Number of surface groups and molecular weights provided by manufacturer. [b]Nanoconstructs were below the detection limit of the instrument. [c]Charge was measured at pH 7.4 (not buffered). [d]Estimation of functional groups was done via titration for OH and NH_2 groups. Results indicate quantity of the corresponding surface-functional group per nanoparticle.

PAMAM dendrimers demonstrated a surface charge and functional group-dependent toxicity profile with amine-terminated dendrimers (both G4 and G7) safely administered only at doses <10 mg/kg. On the contrary, carboxyl (G3.5 and G6.5) and hydroxyl (G4 and G7) terminated dendrimers were safely administered at 50-fold or higher doses. Amine-terminated dendrimers when dosed above their MTDs showed severe abnormalities that are discussed in detail in the following section. In the case of carboxyl- and hydroxyl-terminated dendrimers, the maximum dosage was limited by their solubility in saline. It is interesting that apart from the immediate toxicity (lethality) following injection of doses >10 mg/kg of G4 and G7 amine-terminated dendrimers, animals that survived in these groups showed no clinical signs of toxicity or any significant differences in the blood analysis and histological examinations when compared with control groups. In other words, the animals that survived the immediate toxicity after the administration of

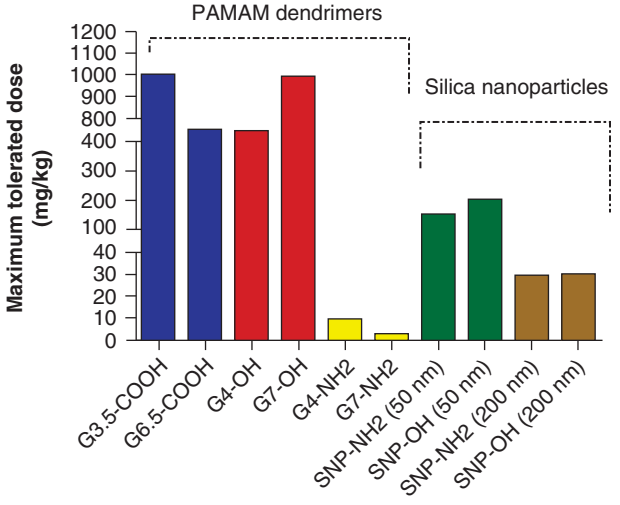

Figure 2. Maximum tolerated doses (MTD) of nanoconstructs in CD-1 mice. A distinct trend was observed in MTD of these nanoparticles as a function of surface charge in the case of dendrimers and size in the case of silica nanoparticles (SNPs). Cationic dendrimers were highly toxic when compared with neutral or negatively charged dendrimers irrespective of their size.

G4-NH_2 and G7-NH_2 amine-terminated dendrimers at doses greater than their respective MTDs were otherwise normal after 10 days of observation. In the case of dendrimers, size variation in the lower nanometre range did not have a significant influence on toxicity because similar patterns were noted for dendritic constructs in the two size ranges studied.

SNPs also showed a clear pattern in the observed *in vivo* toxicity, but unlike the dendrimers, MTD of SNPs was inversely related to their size. The 50-nm SNPs with neutral surface groups were well tolerated for doses of up to 200 mg/kg but doses >200 mg/kg were lethal in CD-1 mice with apparent lung complications probably due to embolization in the lung capillaries. On the other hand, the 200-nm SNPs with hydroxyl surface functionalities were six times less tolerated (30 mg/kg) than the 50-nm counterparts indicating a potential influence of nanoparticle size. The larger SNPs were also in part limited by their stability in aqueous medium. Different surface functionalization of the SNPs did not seem to play a major role in toxicity since the amine-functionalized silica particles had a similar toxicity profile as the corresponding hydroxyl-terminated silica systems used in this study.

Various parameters (ALT, AST, BUN, creatinine, bilirubin and total protein) monitored in plasma after 10 days of acute toxicity studies in mice involving different treatment groups (PAMAM dendrimers and SNPs) did not show any statistical significance from the control groups at respective MTDs. Animal weights monitored twice a day for the period of the acute toxicity study of the various treatment groups at respective MTDs also did not show any significant difference from the control group.

Evidence of disseminated intravascular coagulation-like condition with amine-terminated dendrimers

We further investigated in detail the immediate toxic effects following the administration of amine-terminated dendrimers (G4 and G7) in CD-1 mice. Animals experienced severe reaction to injection (at doses greater than MTD) in 10–20 min manifested by agitation, hyperventilation and lack of activity that warranted animal euthanasia. After euthanasia, necropsy was carried out and blood collection from IVC was attempted, which resulted in only a minimal amount of blood being drawn due to excessive clotting. It is noteworthy that hepatic haemorrhage was observed with these G7-NH_2 dendrimers at doses greater than the MTD of 10 mg/kg (Figure 3A). Intense bleeding in the upper GI tract was also observed (Figure 3B). Extensive concomitant bleeding/clotting phenomena in mice treated with amine-terminated dendrimers was a clinical evidence of disseminated intravascular coagulation-like condition (DIC) and haemolysis (Figure 3C).

These findings indicate haematotoxicity to be the major dose-limiting toxicity observed with G4 and G7 amine-terminated dendrimers. Due to the limited amount of blood that could be drawn for the analysis from mice, we repeated the experiment in SD rats ($n = 3$) where enough blood can be withdrawn for further analysis even in the presence of considerable clotting, 30 min after administration. Blood

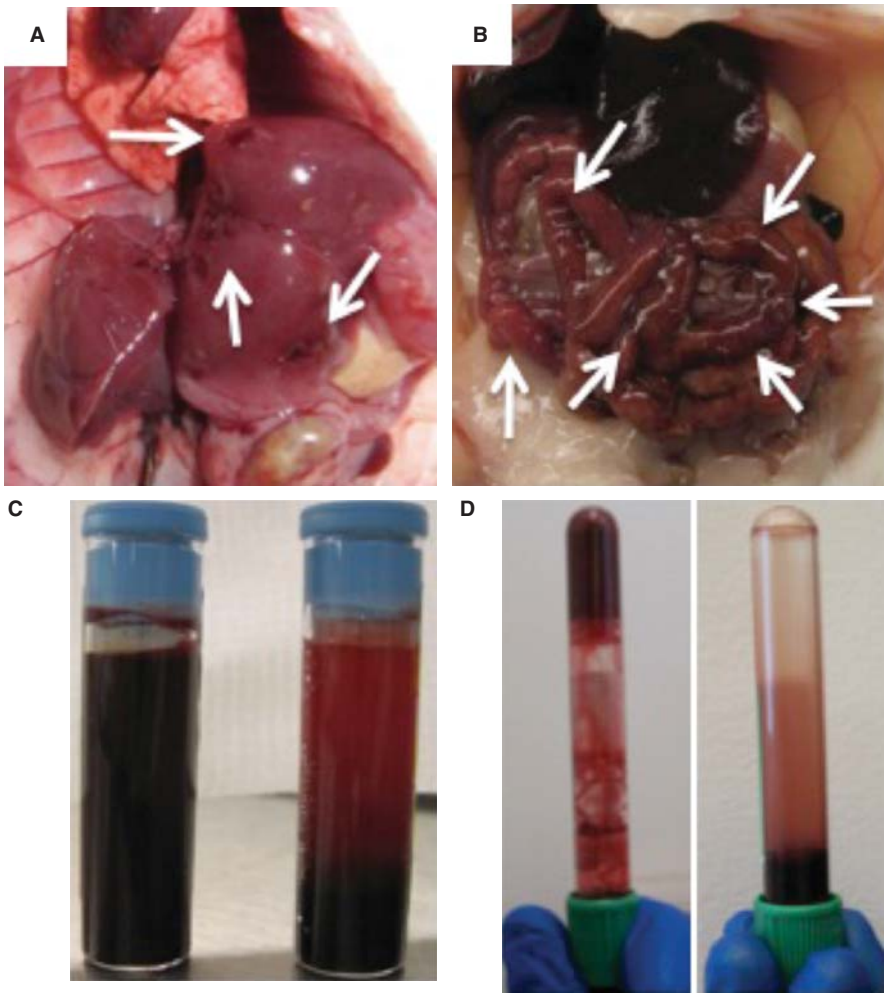

Figure 3. Haematological complication associated with the administration of G7-NH_2 dendrimers. A) Hepatic haemorrhage; B) preferential gastrointestinal haemorrhage; C) haemolysis of mice RBC when compared with control; D) human blood sample showing clotting on the left and control on the right.

analysis showed depleted levels of fibrinogen and high levels of FDPs in groups treated with amine-terminated dendrimers when compared with control groups (Table III). Blood samples collected from these animals also showed significant depletion of platelets (Table III). Human blood samples obtained from donors treated with comparable doses of amine-terminated dendrimers also displayed a similar phenomena with active depletion of fibrinogen and appearance of higher levels of FDPs (Table III, Figure 3D) suggesting the occurrence of both pro- and anti-coagulation processes. This is the first report, to the best of our knowledge, of DIC-like clinical condition observed with the treatment of amine-terminated dendrimers.

Biodistribution of dendrimers correlates with toxicity profile

Biodistribution of the dendritic constructs was further studied to draw correlations with the *in vivo* toxicity results. We again observed a surface-functional group and charge-based trend in the organ distribution of the dendrimers (Figure 4A and Supplementary Figure 2). Amine-terminated dendrimers (G7-NH_2) partitioned out of the blood circulation as early as 2 h and accumulated almost entirely in the liver. On the contrary, carboxyl (G6.5-COOH) and hydroxyl (G7-OH) terminated dendrimers of comparable sizes were retained longer in the blood and slowly excreted via the urine possibly explaining their relative non-toxic nature as observed in the toxicity studies. This trend in biodistribution explains the *in vivo* toxicity data (Figure 3A), which indicate hepatic haemorrhage after G7-NH_2 administration.

To evaluate the dominance of surface charge over nanoparticle size in the range under study, biodistribution of G4-NH_2 was evaluated in comparison with G7-NH_2 (Figure 4A). Despite their significantly smaller size (below renal threshold), G4-NH_2 dendrimers also accumulated in the liver confirming the significant role of protein interactions and opsonization as a consequence of surface charge.

Amine-terminated dendrimers opsonize plasma proteins to a greater extent

In order to explain the differential biodistribution profiles between positively (G7-NH_2) and negatively (G6.5-COOH) charged dendrimers, their tendencies to opsonize plasma proteins was studied. *In vitro* studies in our laboratory showed that positively charged amine-terminated

Table III. Levels of blood coagulation indicators *in vivo* after i.v. administration of nanoconstructs.

Probe (dosed at 30 mg/kg)		Platelets ($\times 10^3/\mu l$) ± S.D.	Haemolysis	Clotting	Fibrinogen level (mg/dl)	Fibrin degradation products (μg/ml)
Animal [a]	Control	453 ± 163	-	-	235 ± 38	<10
	G4-NH_{22}	149 ± 135*	+	++	82 ± 90	>40
	G7-NH_2	129 ± 53*	+	+++	[b]	>40
Human	Control	60 ± 15	–	–	185 ± 30	<10
	G4-NH_2	19.5 ± 0.5*	+	[NA]	<30	>40
	G7-NH_2	25 ± 5*	+	[NA]	[b]	>40

Haemolysis: (+) present, (–) absent; Clotting was scored as following: (++) the ability to withdraw >0.3 ml and <4 ml, (+++) >0.3 ml of blood immediately after euthanasia. [a]Data is for SD rats, as enough samples for the test could not be collected from CD-1 mice. [b]Could not be measured. [NA]Not applicable; however, clotting developed in both G4-NH_2 and G7-NH_2 after the addition of dendrimers to the collected blood from human volunteers, with G7 exhibiting relatively more clotting. *Values are statistically significant compared with the control group.

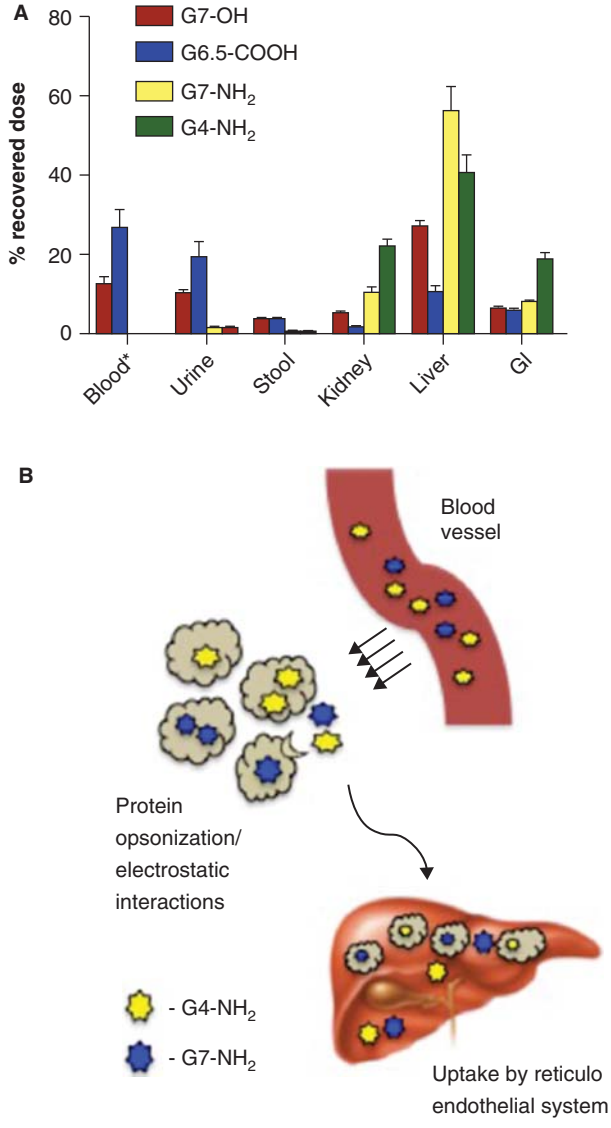

Figure 4. Biodistribution of PAMAM dendrimers at sub-toxic doses 8 h after i.v. administration in CD-1 mice. A) Altering the surface groups on the dendrimer significantly altered the organ localization *in vivo*. Amine-terminated dendrimers accumulated in the liver whereas carboxyl- and hydroxyl-terminated dendrimers were predominantly retained in the blood and excreted via the urine. [#]Radioactivity normalized by weight. B) Cartoon showing amine-terminated dendrimers associate with plasma proteins by opsonization or electrostatic interaction making them susceptible to uptake by reticulo endothelial system in the liver.

dendrimers (G7-NH_2) opsonized albumin (bovine), a model protein, to a greater extent (Supplementary Figure 3) than the carboxyl-terminated negatively charged (G6.5-COOH) dendrimers, suggesting a charge-based differential protein interaction that could potentially lead to distinct biodistribution patterns *in vivo*.

Route of administration affects the toxicity profile

Safety of nanomaterials can also be related to the route of administration. Hence, we further examined the safety of cationic dendrimers administered by oral gavage to CD-1 mice (n = 5). Oral administration of dendrimers resulted in a different toxicity profile than the i.v. route. Two CD-1 mice (out of five) treated with G7-NH_2 at 50 mg/kg showed severe weight loss (>10%) 2 days post-administration. Hence, they were sacrificed and further investigation revealed that the G7-NH_2 dose resulted in fatal haemobilia (Figure 5) whereas G4-NH_2 oral doses of up to 100 mg/kg showed no signs of toxicity 10 days post-oral administration. In contrast, i.v. administration of G4-NH_2 and G7-NH_2 both resulted in severe haematological complications at very low doses. These results suggest that the toxicity profile of amine-terminated PAMAM dendrimers changes significantly with the route of administration.

Discussion

Our results suggest that nanoparticle size seemed to greatly influence the toxicity of silica particles *in vivo*. MTDs of SNPs were inversely related to their size. As the size of SNPs increases, there is a proportional increase in the surface contact area, which could potentially raise the interactions with blood-clotting factors that may lead to embolization ultimately causing toxicity *in vivo*. The possibility of aggregation in small lung capillaries also increases with the size of nanoparticles making this factor dominant for *in vivo* toxicity. This could be the probable reason for the 200-nm SNPs being six times less tolerated (30 mg/kg) than their 50 nm counterparts irrespective of the surface functionalization.

Size of SNPs could potentially have an additional effect on their transport in the vasculature. The 50-nm SNPs could permeate through fenestrations in the blood vessels when compared with the larger 200-nm SNPs, and hence may disrupt blood flow more often. Dendrimers, on the other

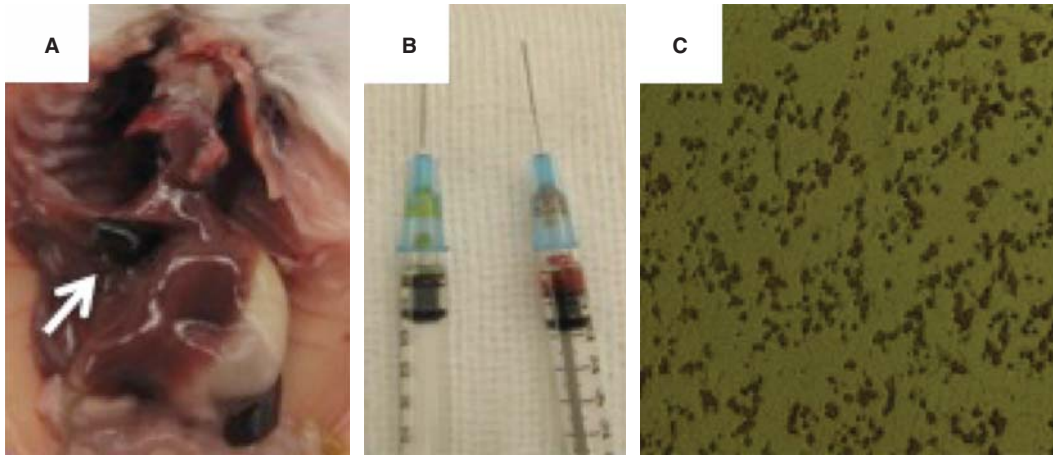

Figure 5. Oral administration of G7-NH_2 at 50 mg/kg in CD-1 mice leads to gall bladder bleeding (haemobilia). A) Gall bladder haemorrhage as indicated by arrow; B) contents of gall bladder aspirated into a 1-ml syringe (red); and contents of a normal gall bladder (green) shown for comparison; C) contents of the gall bladder viewed under an inverted microscope indicating the presence of RBC.

hand, are branched and more flexible nanostructures with hollow spaces between them that will offer minimal resistance to blood flow.

It has been observed by other researchers that only doses as high as 6 mg/mice of mesoporous silicates [Mobil composition of matter (MCM)-41] of size 100–150 nm, injected i.v., resulted in animal death (Hudson et al. 2008). These porous particles seemed to be much more tolerated than our non-porous SNPs possibly because of the way plasma proteins interact with the pores of MCM-41. The biological environment may view porous nanoparticles completely different from a solid particle because the pores allow for different molecular arrangements. Pores of these particles may adsorb a different set of proteins and possibly more proteins are plugged onto the surface exhibiting different conformations that makes them biologically inert and hence lesser toxicity. The influence of protein binding on biocompatibility of SNPs as a function of porosity, size and surface functionality needs further investigation. Other possible explanation could be the agglomeration of SNPs in plasma, which may be inversely related to their size as observed in our case and also witnessed in the maximum solubility of these different sized SNPs.

DIC is a complex systemic thrombo-hemorrhagic disorder involving the generation of intravascular fibrin and consumption of pro-coagulants and platelets. The resultant clinical condition is characterized by intravascular coagulation and haemorrhage as observed in our current experiments with amine-terminated dendrimers. As mentioned in the Results section, we observed hepatic haemorrhage in animals treated with G7-NH_2 at a dose >10 mg/kg. We also observed instestinal haemorrhage probably because of the high blood supply per unit area in the intestine of active feeding animals. DIC has been previously suggested as a possible mode of toxicity associated with nanomaterials *in vivo* (Jeong et al. 2009). To our knowledge, this is the first study to show DIC-like complications after intravenous administration of cationic PAMAM dendrimers.

In order to explain the influence of surface charge and functional group on the toxicity of amine-terminated PAMAM dendrimers (G4-NH_2 and G7-NH_2), we delved into their potential non-specific interactions with elements of the clotting cascade. Blood coagulation is a complex enzymatic event culminating in the formation of an insoluble threadlike fibrin (Furie and Furie 2005) with platelet plugs to prevent excessive bleeding. Activation of fibrinogen (zymogen) into insoluble fibrin monomer is catalysed by the serine protease, thrombin (Hermans & McDonagh 1982). Present in the active site of thrombin is the catalytic triad that cleaves the scissile amide bond on the fibrinogen molecule leading to the generation of fibrin monomers that eventually polymerize to form fibrin clots (Bode 2006; Hermans & McDonagh 1982; Wolberg 2007). Amine-terminated dendrimers that are highly positively charged could mimic the functionality of thrombin in a non-specific fashion and polarize the carbonyl molecule of the scissile amide bond on fibrinogen as suggested in Figure 6A. Carboxyl- or hydroxyl-terminated dendrimers may not be able to cause this polarization of carbonyl moiety by the nature of their surface charge distribution. Under normal physiological conditions, the fibrin blood clots are eventually dissolved in order to restore vascular patency. The central component in the fibrinolytic system is the glycoprotein plasminogen. It is a precursor enzyme that following partial cleavage by activators such as urokinase or tissue plasminogen activator is converted to its proteolytic form, plasmin that cleaves the fibrin clot (Rijken 1988; Vincenza Carriero et al. 2009). As in the case of fibrinogen discussed above, amine-terminated dendrimers could also non-specifically mirror the functioning of urokinase and other plasminogen-activating serine proteases by virtue of their highly positive protonated surface groups generating plasmin, which then degrades the fibrin clots (Figure 6B).

Both fibrinogen and plasminogen precursor molecules that serve different purposes in the clotting cascade could be cleaved by amine-terminated dendrimers essentially by the same process due to the non-specific nature of the interaction between the proteins and positive surface groups of the dendrimers. The biological enzymes (thrombin and urokinase, respectively) involved in these processes are highly specific in recognition and hence do not cross-react, whereas

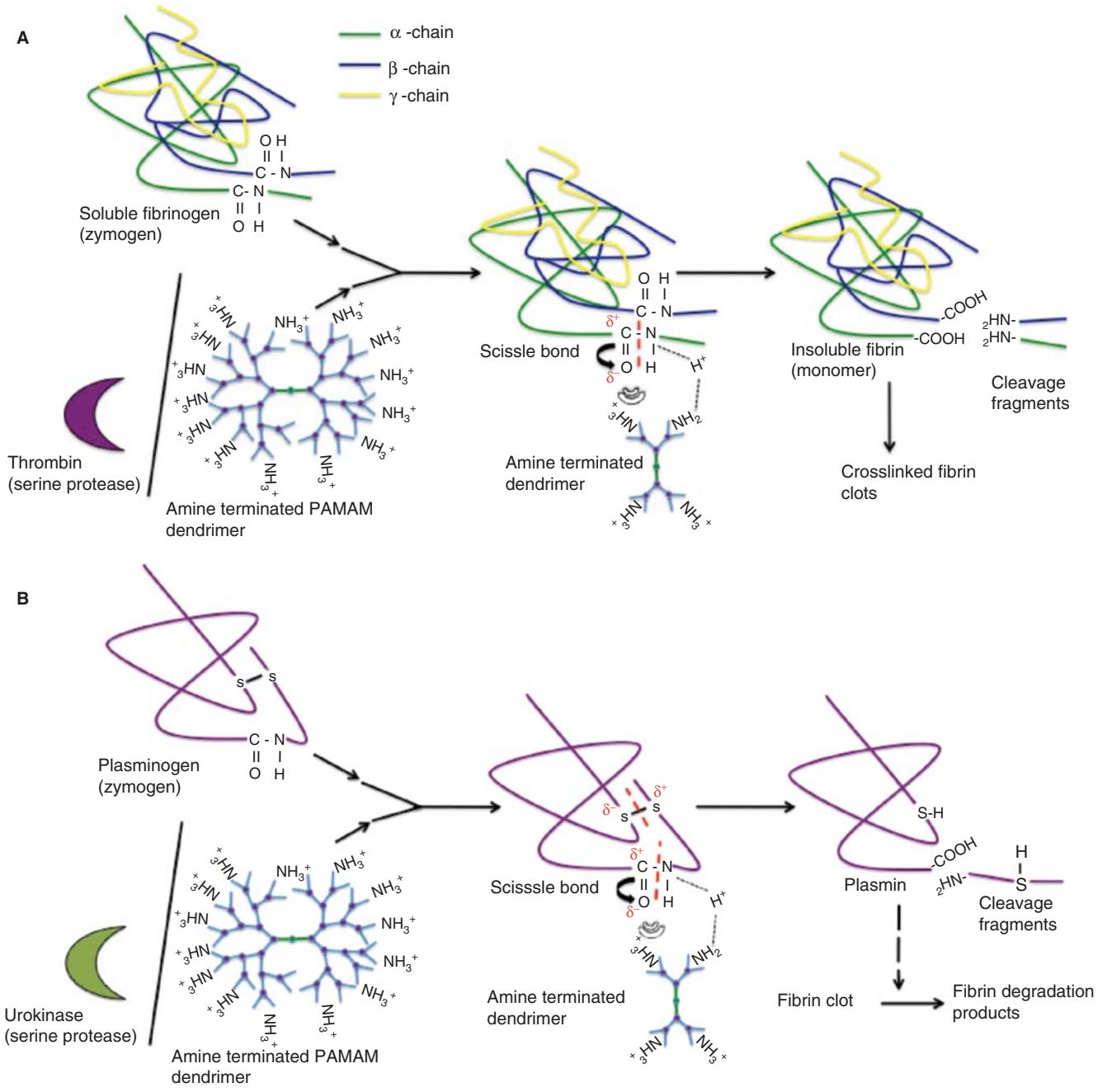

Figure 6. Non-specific cleavage of zymogens by amine-terminated dendrimers in the clotting cascade. A) Proposed mechanism of activation of fibrinogen to fibrin by highly dense positively charged amine-terminated dendrimers through bond polarization to eventually yield insoluble fibrin clots. B) Proposed mechanism of activation of plasminogen to plasmin by highly positively charged amine-terminated dendrimers through bond polarization, which eventually produces fibrin degradation products.

the dendrimers by virtue of their smaller size may be suited to interact with protein active sites and non-specifically initiate both clotting and degradation of clots simultaneously. Our hypothesis correlates well with the observation that there is simultaneous depletion of fibrinogen and high levels of FDPs observed in both animal studies as well as the *ex vivo* human blood experiments (Table III).

It is known that cationic peptides and proteins of lysosomal origin interact extensively with various components of the blood coagulation system (Farbiszewski & Sokol 1988; Saba et al. 1975) causing both plasminogen activator activity and fibrin-polymerizing activity. Previous reports have also alluded to the haemotoxicity of cationic PAMAM dendrimers (Malik et al. 2000); however, the mechanism of such toxicity was not evaluated. The current study clearly implicates plasminogen activator and fibrin-polymerizing activities associated with cationic amine-terminated dendrimers. Recent reports also suggest that fibrin fibres formed in the presence of low thrombin concentration tend to be thick fibres and are easily susceptible to fibrinolysis (Wolberg 2007) as the case would be with amine-terminated dendrimers non-specifically initiating this process.

Interestingly, 200-nm SNPs with comparable zeta potential did not show similar effects. This observed disparity

could be explained in two ways. First, the charge density of amine-terminated dendrimers is much greater than amine-functionalized SNPs. In other words, they have denser accumulation of charges per unit surface area compared with SNPs. For example, assuming that both nanoconstructs are perfect spheres, the surface charge distribution of G7-NH_2 dendrimers (781×10^{-4} mV/nm^2) is approximately 600-fold higher when compared with the 200-nm amine-functionalized SNPs (1.22×10^{-4} mV/nm^2). The second factor could be that the smaller size and symmetrical charge distribution of PAMAM dendrimers with uniform spacing between adjacent amine groups may act as an efficient system for tertiary configuration alignments with proteins such as fibrinogen and plasminogen, whereas the random surface group alignment on SNPs and larger particle size may not be favourable for such interactions. Surface charge distribution and their density on nanoconstructs play a significant role in biological interactions probably more so than composition or total charge itself in the studied range.

The two studied nanostructures (PAMAM dendrimers and SNPs) exhibited distinctly different trends on toxicity either based on size or surface charge but the composition of SNPs and PAMAM dendrimers could also play a role in the observed toxicity *in vivo*. It is evident that out of the 10 nanoconstructs tested, amine-terminated dendrimers were the least tolerated (10 mg/kg), which limits the utility of higher generation cationic dendrimers in drug delivery. Partial surface modifications of these cationic dendrimers, however, have shown to reduce their toxicity and render them suitable for biological applications (Kolhatkar et al. 2007). Hence, surface capping is a possibility if the use of these systems is inevitable in specific applications.

Results from the biodistribution of PAMAM dendrimers showed that amine-terminated dendrimers mostly accumulated in the liver, whereas carboxyl- and hydroxyl-terminated dendrimers tend to remain in the blood circulation for longer. Positively charged dendrimers could potentially interact to a greater extent with plasma proteins resulting in a larger size (Gabellieri et al. 2006; Klajnert et al. 2003) as well as rendering the protein–dendrimer complex susceptible to clearance by the reticulo-endothelial system in the liver (Figure 4B). Our *in vitro* protein opsonization studies ('Amine-terminated dendrimers opsonize plasma proteins to a greater extent' section) also further confirm this fact. Both G4-NH_2 dendrimers, which are sized below the renal threshold, and G7-NH_2 dendrimers, sized above the renal threshold, accumulate in the liver irrespective of their size because of plasma–protein interactions possibly suggesting that surface charge plays a more dominant role than size with respect to biodistribution of these specific nanoconstructs under study. Furthermore, these dendrimers started to appear in the stool and GI tract over time (Figure 4A and Supplementary Figure 2). Dendrimers acquiring larger size by protein interactions could possibly cross the liver fenestration and be uptaken by hepatocytes, thus accumulating in the stool through bile secretions as observed with other nanoparticles (Souris et al. 2010).

Oral administration of G7-NH_2 dendrimers at 50 mg/kg showed fatal occurrence of haemobilia. This finding indicates possible translocation of G7-NH_2 across the intestinal epithelium and subsequent uptake by hepatocytes and secretion through the bile fluid into the gall bladder. In contrast, oral administration of G4-NH_2 at 100 mg/kg showed no apparent signs of toxicity. One possible explanation is that cationic G4 dendrimers have a lesser surface charge density when compared with G7, which could enable opening of the tight junctions in the intestine. Hence, lesser G4 dendrimers are transported across the intestine into the blood stream when compared with G7 dendrimers.

Conclusions

In conclusion, our study indicates distinct differences in the *in vivo* toxicity of PAMAM dendrimers and SNPs as a function of surface charge and size. In addition to these factors, surface charge density and composition of nanomaterials were shown to influence biological interactions. Amine-terminated dendrimers caused haematotoxicity by a complex and dynamic process such as DIC, which we report here for the first time. Employment of amine-terminated dendrimers in human applications can potentially prove fatal unless their surface properties are modified to reduce toxic effects. Results have significant implications for use of these materials in imaging, diagnostics, drug delivery, theranostics and other biomedical applications where knowledge about the maximum dose that can be safely administered is crucial.

Acknowledgements

Financial support was provided by NIH Grants (R01DE019050 and R01EB07470) and the Utah Science Technology and Research (USTAR) initiative.

Declaration of interest

The authors report no conflicts of interest. The authors alone are responsible for the content and writing of the paper.

References

Aillon KL, Xie Y, El-Gendy N, Berkland CJ, Forrest ML. 2009. Effects of nanomaterial physicochemical properties on in vivo toxicity. Adv Drug Deliv Rev 61:457–466.

Bode W. 2006. Structure and interaction modes of thrombin. Blood Cells Mol Dis 36:122–130.

Esfand R, Tomalia DA. 2001. Poly(amidoamine) (PAMAM) dendrimers: from biomimicry to drug delivery and biomedical applications. Drug Discov Today 6:427–436.

Farbiszewski R, Sokol A. 1988. The interaction between fibrinogen and 3H-L-arginine cationic peptides derived from fibrosarcoma in the presence of thrombin. Haematologia (Budap) 21:169–173.

Fischer HC, Chan WC. 2007. Nanotoxicity: the growing need for in vivo study. Curr Opin Biotechnol 18:565–571.

Fruijtier-Polloth C. 2005. Safety assessment on polyethylene glycols (PEGs) and their derivatives as used in cosmetic products. Toxicology 214:1–38.

Furie B, Furie BC. 2005. Thrombus formation in vivo. J Clin Invest 115:3355–3362.

Gabellieri E, Strambini GB, Shcharbin D, Klajnert B, Bryszewska M. 2006. Dendrimer-protein interactions studied by tryptophan room

temperature phosphorescence. Biochim Biophys Acta 1764:1750–1756.
Hardman R. 2006. A toxicologic review of quantum dots: toxicity depends on physicochemical and environmental factors. Environ Health Perspect 114:165–172.
Hermans J, McDonagh J. 1982. Fibrin: structure and interactions. Semin Thromb Hemost 8:11–24.
Hudson SP, Padera RF, Langer R, Kohane DS. 2008. The biocompatibility of mesoporous silicates. Biomaterials 29(30):4045–4055.
Jeong J, Cho W-S, Kim SH, Cho M-H. 2009. In Vitro and In Vivo Toxicity Study of Nanoparticles: John Wiley & Sons, Ltd. pp 303–334.
Klajnert B, Stanislawska L, Bryszewska M, Palecz B. 2003. Interactions between PAMAM dendrimers and bovine serum albumin. Biochim Biophys Acta 1648:115–126.
Kolhatkar RB, Kitchens KM, Swaan PW, Ghandehari H. 2007. Surface acetylation of polyamidoamine (PAMAM) dendrimers decreases cytotoxicity while maintaining membrane permeability. Bioconjug Chem 18:2054–2060.
Lin W, Huang YW, Zhou XD, Ma Y. 2006. In vitro toxicity of silica nanoparticles in human lung cancer cells. Toxicol Appl Pharmacol 217:252–259.
Malik N, Wiwattanapatapee R, Klopsch R, Lorenz K, Frey H, Weener JW, et al. 2000. Dendrimers: relationship between structure and biocompatibility in vitro, and preliminary studies on the biodistribution of 125I-labelled polyamidoamine dendrimers in vivo. J Control Release 65:133–148.
Nel A, Xia T, Madler L, Li N. 2006. Toxic potential of materials at the nanolevel. Science 311:622–627.
Rijken DC. 1988. Relationships between structure and function of tissue-type plasminogen activator. Klin Wochenschr 66 Suppl 12:33–39.
Saba HI, Herion JC, Walker RI, Roberts HR. 1975. Effect of lysosomal cationic proteins from polymorphonuclear leukocytes upon the fibrinogen and fibrinolysis system. Thromb Res 7:543–554.
Service RF. 1995. Dendrimers: dream molecules approach real applications. Science 267:458–459.
Souris JS, Lee CH, Cheng SH, Chen CT, Yang CS, Ho JA, et al. 2010. Surface charge-mediated rapid hepatobiliary excretion of mesoporous silica nanoparticles. Biomaterials 31:5564–5574.
Stober W, Fink A, Bohn E. 1968. Controlled growth of monodisperse silica spheres in the micron size range. J Colloid Interface Sci 26:62–69.
Svenson S, Tomalia DA. 2005. Dendrimers in biomedical applications–reflections on the field. Adv Drug Deliv Rev 57:2106–2129.
Tomalia DA. 1994. Starburst/cascade dendrimers: fundamental building blocks for a new nanoscopic chemistry set. Adv Mater 6:529–539.
Tomalia DA, Naylor AM, Goddard WA. 1990. Starburst dendrimers: molecular-level control of size, shape, surface chemistry, topology, and flexibility from atoms to macroscopic matter. Angew Chem Int Ed Engl 29:138–175.
Van Blaaderen A, Vrij A. 1992. Synthesis and characterization of colloidal dispersions of fluorescent, monodisperse silica spheres. Langmuir 8:2921–2931.
Vincenza Carriero M, Franco P, Vocca I, Alfano D, Longanesi-Cattani I, Bifulco K, et al. 2009. Structure, function and antagonists of urokinase-type plasminogen activator. Front Biosci 14:3782–3794.
Weetall HH. 1993. Preparation of immobilized proteins covalently coupled through silane coupling agents to inorganic supports. Appl Biochem Biotechnol 41:157–188.
Wilbur DS, Pathare PM, Hamlin DK, Buhler KR, Vessella RL. 1998. Biotin reagents for antibody pretargeting. 3. Synthesis, radioiodination, and evaluation of biotinylated starburst dendrimers. Bioconjug Chem 9:813–825.
Wolberg AS. 2007. Thrombin generation and fibrin clot structure. Blood Rev 21:131–142.

Supplementary material available online

Figures 1–3 and Tables I and II